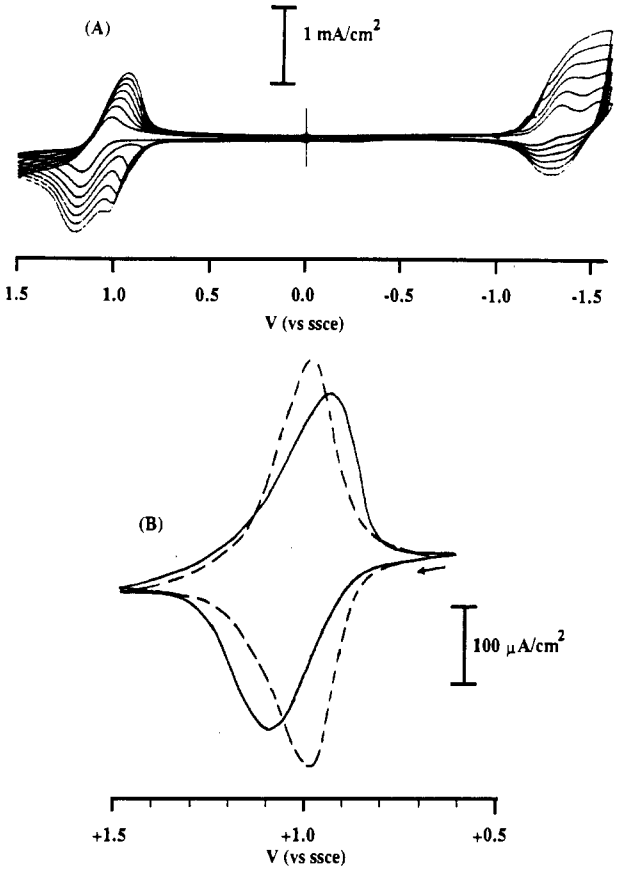

Figure 4. (A) Consecutive cyclic voltammetric traces for $[Fe(vbpy)_3]^{2+}$ in 0.1 M TBAH/DFB at a 0.1 cm^2 Pt electrode at a sweep rate of 100 mV/s, illustrating polymeric film growth by electropolymerization. (B) Cyclic voltammograms of the Fe(III/II) couple in the polymeric $[Fe(vbpy)_3]^{2+}$ film from part A at 50 mV/s when immersed in 0.1 M TBAH solutions of DFB (—) and CH_3CN (---).

As examples, we have studied the reductive electropolymerizations of $[Fe(vbpy)_3]^{2+}$ and $[Re(vbpy)(CO)_3Cl]$, both of which have been studied previously in CH_3CN.[13,14] The rate of electropolymerization of $[Fe(vbpy)_3]^{2+}$ in DFB (Figure 4A) is comparable to that in CH_3CN as judged by the increase in peak currents for the film-based couples on sequential scanning. Cyclic voltammetric traces of a polymeric $[Fe(vbpy)_3]^{3+/2+}$ film in DFB and CH_3CN are shown in Figure 4B. At a sweep rate of 50 mV/s, the peak-to-peak splitting for the Fe(III/II) couple is 200 mV in DFB while it is only 35 mV in CH_3CN, showing that charge propagation through the film is considerably slower in DFB. As an electropolymerization solvent, DFB has proven to be especially valuable for the electropolymerization of $[Re(vbpy)(CO)_3Cl]$, the details of which have been described in detail in CH_3CN elsewhere.[6,14] As a solvent, it offers the advantages that the resulting films are much more stable toward reductive cycling and that electropolymerization onto optically transparent In-doped SnO_2 electrodes yields much more uniform coverages at a considerably enhanced rate.[15]

1,2-Difluorobenzene is also a useful solvent for oxidative electropolymerizations. We have studied the oxidative electropolymerization of Fe(PPIX-dme)Cl (PPIX-dme = protoporphyrin IX dimethyl ester), which can be carried out on carbon, Pt, and In-doped SnO_2 electrodes. Films of polymeric [Fe(PPIX-dme)Cl] were prepared by cycling the applied potential between 0.0 and +1.3 V at a sweep rate of 100 mV/s in 0.1 M TBAH/DFB. The electropolymerization proceeds more rapidly and reproducibly in DFB than in DMF, CH_2Cl_2, or CH_3CN,[16,17] and it is possible to

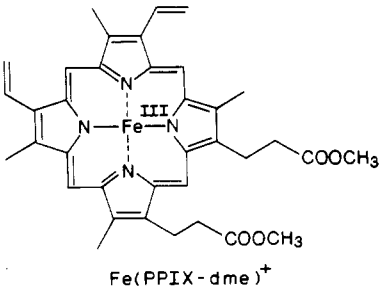

Fe(PPIX-dme)$^+$

grow films that are thicker by factors of 10 or greater. This porphyrin also undergoes slow *reductive* electropolymerization in DFB by scanning between 0.0 and −1.6 V. Of the four solvents, DFB, DMF, CH_2Cl_2, or CH_3CN, reductive electropolymerization only occurs in DFB.[17]

Acknowledgment. Funding from the Office of Naval Research and the National Institutes of Health for support of J.N.Y. (Postdoctoral Fellowship No. 1-F32-GM11280-01A1) is gratefully acknowledged.

Registry No. DFB, 367-11-3; TBAH, 3109-63-5; Pt, 7440-06-4; C, 7440-44-0; In-Sn-O, 50926-11-9; $[Fe(bpy)_3]^{3+}$, 18661-69-3; $[Fe(bpy)_3]^{2+}$, 15025-74-8; $[Fe(\eta^5\text{-}Me_5C_5)_2]^+$, 54182-41-1; $[Fe(\eta^5\text{-}Me_5C_5)_2]$, 12126-50-0; $[Re(bpy)(CO)_3Cl]$, 52064-98-9; $[Re(bpy)(CO)_3Br]$, 56498-59-0; $[Re(bpy)(CO)_3CF_3SO_3]$, 97170-94-0; $[Re(bpy)(CO)_3(CH_3CN)]^+$, 89708-63-4; $[(CO)_5Re\text{-}Re(bpy)(CO)_3]$, 61993-42-8; $[(CO)_3(bpy)Re\text{-}Re(bpy)(CO)_3]$, 107228-01-3; $[Fe(vbpy)_3]^{2+}$, 75675-26-2; $[Re(vbpy)(CO)_3Cl]$, 100243-94-5; Fe(PPIX-dme)Cl, 15741-03-4.

(15) O'Toole, T. R.; Sullivan, B. P.; Meyer, T. J. *J. Am. Chem. Soc.*, in press.
(16) Dong, S.; Jiang, R. *J. Inorg. Biochem.* **1987**, *30*, 189.
(17) Younathan, J. N.; Wood, K.; Rhodes, M.; Meyer, T. J. Manuscript in preparation.
(18) *Electrochemical Methods*; Bard, A. J., Faulkner, L. R., Eds.; Wiley: New York, 1980.

Contribution from the Department of Chemistry, University of Minnesota, Minneapolis, Minnesota 55455

Preferential Solvation Effects Observed in a Kinetic Study of the Reaction of $[(\eta^6\text{-}C_6Me_6)Ru(\eta^6\text{-anth})][PF_6]_2$ with Acetonitrile (anth = Anthracene)

Daniel A. Freedman and Kent R. Mann*

Received March 15, 1989

Recently our group described kinetic measurements on the reaction of a series of $[CpRu(\eta^6\text{-arene})]^+$ and $[Cp^*Ru(\eta^6\text{-arene})]^+$ complexes (Cp = η^5-cyclopentadienyl; Cp* = η^5-pentamethylcyclopentadienyl) with acetonitrile to give free arene and the corresponding tris(acetonitrile) compound.[1] Rate data for the reaction with $[Cp^*Ru(anth)]^+$ (anth = η^6-anthracene) were acquired at different temperatures and acetonitrile concentrations. As a continuation of our inquiry in this area, we have studied the analogous bis(arene) complex $[(HMB)Ru(anth)]^{2+}$ (HMB = η^6-hexamethylbenzene).

Bennett et al. reported that the bis(arene) compound $[(mes)Ru(anth)]^{2+}$ (mes = η^6-mesitylene) undergoes a facile, thermal reaction with DMSO to yield the tris-DMSO complex (reaction 1).[2] We have shown that $[(HMB)Ru(anth)]^{2+}$ reacts similarly

$$[(mes)Ru(anth)]^{2+} + 3DMSO \rightarrow [(mes)Ru(DMSO)_3]^{2+} + anthracene \quad (1)$$

with acetonitrile (reaction 2). The kinetic investigation of reaction

$$[(HMB)Ru(anth)]^{2+} + 3CH_3CN \rightarrow [(HMB)Ru(CH_3CN)_3]^{2+} + anthracene \quad (2)$$

2 was undertaken in two solvent systems, acetonitrile/methylene

* To whom correspondence should be addressed.

0020-1669/89/1328-3926$01.50/0

chloride and acetonitrile/nitromethane, to discern the possible mechanisms for arene release from this bis(arene) complex. We observe a saturation effect at high concentrations of CH_3CN in CH_2Cl_2, but not when the more polar CH_3NO_2 is the solvent. A nonlinear shift of the HMB ^1H chemical shifts in the complex with $[CH_3CN]$ in CH_2Cl_2 indicates that the probable cause of the saturation effect is the preferential solvation of $[(HMB)Ru(anth)]^{2+}$ by CH_3CN solutions.

Experimental Section

General Considerations. All synthetic procedures were carried out under an inert N_2 atmosphere unless otherwise noted. Solvents used were of spectroscopic grade and were used without further purification except in the case of the kinetic measurements where acetonitrile, methylene chloride, and nitromethane were distilled from P_2O_5 prior to use. ^1H NMR spectra were recorded on a IBM AC-200 NMR spectrometer. Chemical shifts are relative to $(CH_3)_4Si$. UV–vis spectra were recorded on a Cary 17D spectrometer equipped with computer control. Elemental analyses were performed by MHW Laboratories. $[RuCl_2(HMB)]_2$ was prepared by a literature procedure.[3,4]

Compound Synthesis. [(HMB)Ru(anth)][PF_6]$_2$. Silver hexafluorophosphate (76 mg, 0.301 mmol) was added to a solution of 50 mg (0.075 mmol) of $[RuCl_2(HMB)]_2$ in 10 mL of acetone. After the solution was stirred for 15 min, the precipitated silver chloride was filtered off to leave a light yellow solution. The acetone was removed by rotary evaporation to yield a light yellow oil. Trifluoroacetic acid (5 mL) and an excess of anthracene (0.200 g) were added, and the solution was refluxed for 20 min to give a dark red-purple solution. The trifluoacetic acid was removed by rotary evaporation, and a small amount of ice water was added. The intense red solution was then filtered into an ice water solution of ammonium hexafluorophosphate to give a bright orange precipitate, which was filtered. The orange precipitate was dissolved in acetone, reprecipitated with ether, and then filtered and washed with ether to yield 54 mg of bright orange microcrystals (49% yield). Anal. Calcd for $C_{22}H_{32}RuP_2F_{12}$: C, 42.69; H, 3.87. Found: C, 42.73; H, 4.00. ^1H NMR (200 MHz, acetone-d_6): 2.261 (s, C_6Me_6, 18 H), 7.232 (d of d, $H_{2,3}$, 2 H, J_{vic} = 4.6 Hz, $J_{allylic}$ = 2.6 Hz), 7.903 (d of d, $H_{1,4}$, 2 H, J_{vic} = 6.8 Hz, $J_{allylic}$ = 3.2 Hz), 8.046 (d of d, $H_{6,7}$, 2 H, J_{vic} = 2.6 Hz, $J_{allylic}$ = 4.6 Hz), 8.292 (d of d, $H_{5,8}$, 2 H, J_{vic} = 6.8 Hz, $J_{allylic}$ = 3.2 Hz), 8.975 (s, $H_{9,10}$, 2 H).

Measurement of Kinetic Parameters. Absorption changes at 510 nm were measured during the course of reaction 2 as a function of time. Sampling was controlled through computer software designed for this purpose. A small (approximately 2 mg) sample of the complex was added to a 1-cm quartz cell equipped with a serum stopper. Due to the low solubility of [(HMB)Ru(anth)](PF_6)$_2$ in methylene chloride, it was necessary to use a 5-cm cell to provide sufficient absorbance at low concentrations of acetonitrile. A stock solution of acetonitrile in either methylene chloride or nitromethane was introduced by syringe while the cell was in the cell holder. Timing of the reaction was begun at the addition of the solution followed by thorough shaking of the mixture to ensure adequate mixing. All manipulations were carried out in the absence of light.

The value of k_{obs} for each experiment was determined by least-squares evaluation of a plot of ln $(A_t - A_f)/l$ vs time according to eq 3, where

$$\ln [(A_t - A_f)/l] = \ln [(\epsilon_i - \epsilon_f)C_0] - k_{obs}t \quad (3)$$

A_t = absorption at time t, A_f = absorbance at infinity, l = path length of cell, ϵ_i = extinction coefficient of reactants at monitoring wavelength, and ϵ_f = extinction coefficient of products at monitoring wavelength. All plots based on eq 3 (typically 100–200 data points) were linear through at least 6 half-lives. All the data points were given equal weighting. The precision of the rate constants reported here is ±8%. Reproducible data were only obtained when the solvents were rigorously dryed.

The temperature of the solution was kept at a constant 25 ± 0.5 °C during the kinetic runs. Cells, stock solutions, and acetonitrile were equilibrated in a circulating bath of ethylene glycol for at least $^1/_2$ h before introduction to the cell holder. The temperature of the cell was controlled (±0.5 °C) by circulating the thermostated solvent mixture through a cell holder filled with water. Temperatures were monitored with a copper–constantan thermocouple immersed in the solutions.

To ensure that no secondary processes occurred during the time period of the experiments, parallel experiments were performed in the unreactive pure solvents, methylene chloride and nitromethane. Only slight variations in absorbance due to variations introduced by the sampling techniques were observed.

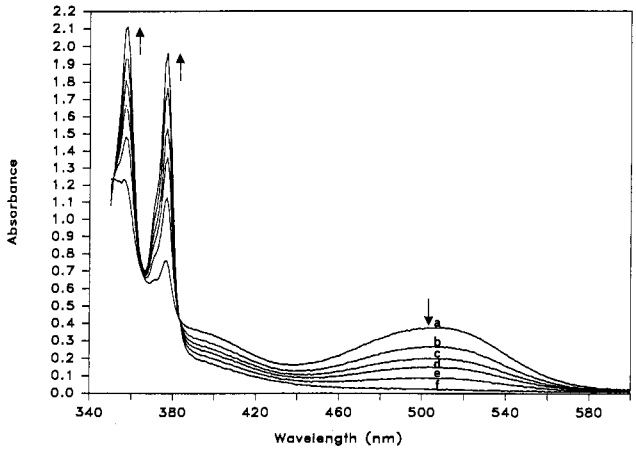

Figure 1. UV–vis spectral changes that occur during the reaction of $\sim 10^{-3}$ M $[(HMB)Ru(anth)]^{2+}$ with 5.47 M CH_3CN in CH_2Cl_2. Arrows indicate the direction of the absorbance changes with time. Spectra were taken at the following times: a, t = 0 min; b, t = 6 min; c, t = 12 min; d, t = 18 min; e, t = 30 min; f, t = 68 min.

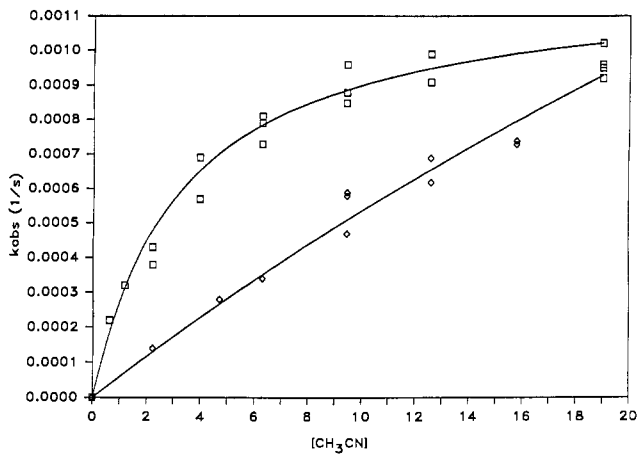

Figure 2. Plots of k_{obs} vs $[CH_3CN]$ for the reaction of [(HMB)Ru(anth)][PF_6]$_2$ in CH_2Cl_2 (□) and CH_3NO_2 (◇). The nonlinear least-squares line is drawn through the CH_2Cl_2 data according to eq 3 with K = 0.30 (4) M^{-1} and k_2 = 0.0012 (1) s^{-1}. The line drawn through the CH_3NO_2 data has K = 0.012 (7) M^{-1} and k_2 = 0.005 (2.7) s^{-1}.

Results and Discussion

[(HMB)Ru(anth)][PF_6]$_2$ was synthesized from $[RuCl_2(HMB)]_2$ by a slight modification of the route developed by Bennett.[3] The compound was characterized by ^1H NMR and elemental analysis. The anthracene region of the ^1H NMR spectrum of $[(HMB)Ru(anth)]^{2+}$ is very similar to that of the Cp* analogue[1] and shows the characteristic upfield shift of the protons on the ring bound to the metal.[4] The pattern of anthracene ^1H resonances is clearly consistent with η^6-coordination to one of the outer rings as is the case for the Cp* analogue.

Kinetic measurements for reaction 1 were made by monitoring changes in the UV–vis spectra. The clean, isosbestic behavior that occurs in the UV–vis spectrum for one trial is shown in Figure 1. Rate data as a function of $[CH_3CN]$ were determined by monitoring the absorbance at one wavelength (510 nm) as a function of time. Two different solvent systems were used for the kinetic studies—acetonitrile/nitromethane and acetonitrile/methylene chloride.

The k_{obs} vs $[CH_3CN]$ plots for both solvents are shown in Figure 2. The rates in both pure solvent systems are essentially zero (no observable reaction in either pure nitromethane or methylene

(1) McNair, A. M.; Mann, K. R. *Inorg. Chem.* **1986**, *25*, 2519.
(2) Bennett, M. A.; Matheson, T. W. *J. Organomet. Chem.* **1979**, *175*, 87.
(3) Bennett, M. A.; Matheson, T. W.; Robertson, G. B.; Smith, A. K.; Tucker, P. A. *Inorg. Chem.* **1980**, *19*, 1014.
(4) (a) For a review see: Sutherland, R. G.; *J. Organomet. Chem. Libr.* **1977**, *3*, 311. (b) Vol'kenau, N. A.; Bolesova, I. N.; Shul'pina, L. S.; Kitaigorodskii, A. N.; Kravtsov, D. N. *J. Organomet. Chem.* **1985**, *288*, 341.

Table I. Concentration Study of the Kinetics of the Reaction of $[(HMB)Ru(\eta^6\text{-anth})][PF_6]_2$ with CH_3CN

CH_2Cl_2 as the solvent		CH_3NO_3 as the solvent	
$[CH_3CN]$, M	10^4k_{obs},[a] s^{-1}	$[CH_3CN]$, M	10^4k_{obs}, s^{-1}
0.611	2.2	2.22	1.4
1.18	3.2	4.70	2.8
2.23	4.1	6.30	3.4
3.98	6.3	9.46	5.5
6.30	7.8	12.6	6.6
9.46	9.0	15.8	7.4
12.6	9.5	6.4[c]	3.3
19.0	9.6	6.4[d]	2.8
6.4[b]	7.0		
19.0[b]	8.4		

[a] The estimated error in the rate constants is ±8%. [b] Determined in the presence of 0.10 M $(TBA)PF_6$. [c] Determined in acetone. [d] Determined in propylene carbonate.

chloride) while the upper limit for both systems is the rate in pure acetonitrile. It is of interest that the rate increases almost linearly with acetonitrile concentration in nitromethane solutions while in methylene chloride the rate reaches a limiting value at ca. 10 M acetonitrile. No effect was observed when tetra-*n*-butyl ammonium hexafluorophosphate was added to the CH_2Cl_2 solutions. The values for k_{obs} at different acetonitrile concentrations are given in Table I. The linear variation of k_{obs} with $[CH_3CN]$ in nitromethane is consistent with an overall second-order rate law for anthracene displacement (first order in complex and first order in acetonitrile) with an apparent second-order rate constant of 4.8×10^{-5} M^{-1} s^{-1}.

There are two mechanisms that we considered to account for these data. The first was similar to one of the mechanisms proposed for the reaction of $[Cp^*Ru(anth)]^+$ with acetonitrile.[1] A rapid preequilibrium is established between the starting complex and an η^4-arene complex with one acetonitrile molecule in the coordination sphere.[1] First-order release of the η^4-arene from this complex followed by the rapid addition of two additional acetonitrile molecules completes the reaction:

$$[(HMB)Ru(\eta^6\text{-anth})]^{2+} + CH_3CN \underset{}{\overset{K}{\rightleftharpoons}} [(HMB)Ru(\eta^4\text{-anth})(CH_3CN)]^{2+} \quad (4)$$

$$[(HMB)Ru(\eta^4\text{-anth})(CH_3CN)]^{2+} \xrightarrow[2CH_3CN]{k_2} [(HMB)Ru(CH_3CN)_3]^{2+} + anth \quad (5)$$

The rate equation for this scheme is

$$k_{obs} = \frac{k_2K[CH_3CN]}{1 + K[CH_3CN]} \quad (6)$$

This equation requires a saturation effect at high concentrations of acetonitrile when the decomposition of the η^4-arene complex becomes rate determining. A nonlinear least-squares fit of the data to eq 6 yields the line drawn through the methylene chloride data in Figure 2. The parameters that give the best fit are K = 0.30 (4) M^{-1} and k_2 = 0.0012 (1) s^{-1}. The fit appears quite good, but we believe that this *particular* preequilibrium mechanism can be ruled out for several reasons. First, the mechanism does not explain why saturation is observed in CH_2Cl_2 and not in CH_3NO_2. The nitromethane data were also fit with eq 1 to yield the parameters K = 0.012 (7) M^{-1} and k_2 = 0.005 (2.7) s^{-1}. We can think of no reasonable way to account for the decrease by a factor of 25 of the equilibrium constant for the "ring slip" preequilibrium, a process that should not exhibit a large solvent effect. Further, no evidence of the slipped-ring intermediate is observed in the ^1H NMR spectrum[5] or in the UV–vis spectrum[6] of the complex in

Table II. ^1H NMR Study of the Shift of the HMB Peak in $[(HMB)Ru(\eta^6\text{-anth})][PF_6]_2$ Relative to $[CD_3CN]$ in CD_2Cl_2 and CD_3NO_2 Solutions

$[CD_3CN]$,[a] M	peak position,[b] ppm	normalized shift $(\delta_{solv} - \delta)/(\delta_{solv} - \delta_{CH_3CN})$
	HMB Peak Position in CD_2Cl_2	
19.2	2.011	1.000
15.3	2.025	0.868
11.5	2.033	0.793
7.66	2.044	0.689
3.83	2.060	0.538
1.92	2.078	0.377
0.96	2.091	0.245
0.77	2.093	0.226
0.00	2.117	0.000
	HMB Peak Position in CD_3NO_2	
19.2	2.011	1.000
15.1	2.041	0.829
11.3	2.070	0.663
7.27	2.106	0.457
3.91	2.144	0.240
0.00	2.186	0.000

[a] $[CH_3CN]$ are ±5%. [b] Peak positions are ±0.001 ppm.

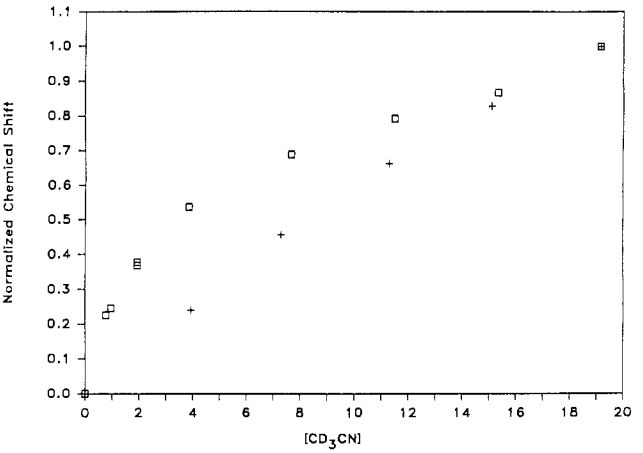

Figure 3. Plots of the normalized ^1H NMR shift $((\delta_{solv} - \delta)/(\delta_{solv} - \delta_{CH_3CN}))$ for the HMB resonance vs $[CD_3CN]$ in CD_2Cl_2 (□) and CD_3NO_2 (+).

CH_2Cl_2/CH_3CN solutions, although the K value of 0.30 M^{-1} suggests a significant amount of the ring-slipped intermediate should be present.

An alternative possibility explains the solvent effect if saturation occurs because the highly polar, dicationic metal complex is preferentially solvated by the acetonitrile in the low dielectric methylene chloride solution but to a much lesser extent in nitromethane.[7] *Specific* interactions with nitromethane can be ruled out because the rates of reaction with 6.4 M $[CH_3CN]$ in other high dielectric solvents (acetone and propylene carbonate) are nearly identical with the nitromethane rate. In effect, the concentration of acetonitrile in the solvation sphere of the metal

(5) This argument is equivocal if the interconversion rate between the η^6 and η^4 complexes is fast ($\sim 10^3$ s^{-1}) on the ^1H NMR time scale. ^1H NMR spectra of $[(HMB)Ru(anth)]^{2+}$ in CD_3CN/CH_2Cl_2 mixtures do not show any evidence for separate η^6–η^4-coordinated anthracene peaks down to −68 °C.

(6) The UV–VIS spectra of $[(HMB)Ru(anth)]^{2+}$ are nearly identical in CH_3CN and CH_2Cl_2 with λ_{max} = 511 nm in CH_3CN and λ_{max} = 515 nm in CH_2Cl_2.

(7) Preferential solvation papers: (a) Detellier, C.; Gerstmans, A.; Laszlo, P. *Inorg. Nucl. Chem. Lett.* **1979**, *15*, 93. (b) Gustavsson, H.; Ericsson, T.; Lindman, B. *Inorg. Nucl. Chem. Lett.* **1978**, *14*, 37. (c) Greenberg, M. S.; Popov, A. I. *Spectrochem. Acta* **1975**, *31A*, 697. (d) Dechter, J. J.; Zink, J. I. *Inorg. Chem.* **1976**, *7*, 1690. (e) Nagy, O. B.; Muanda, M. W.; Nagy, J. B. *J. Chem. Soc., Faraday Trans. 1* **1978**, *74*(9), 2210. (f) Beguin, C.; Delpuech, J. J.; Peguy, A. *Mol. Phys.* **1969**, *17*, 317. (g) Covington, A. K.; Thain, J. M. *J. Chem. Soc. Faraday Trans. 1* **1974**, *70*, 1879. (h) Covington, A. K.; Lantzke, I. R.; Thain, J. M. *J. Chem. Soc., Faraday Trans. 1* **1974**, *70*, 1869. (i) Frankel, L. S.; Langford, C. H.; Stengle, T. R. *J. Phys. Chem.* **1970**, *74*, 1376. (j) Bertran, J. F.; Rodriguez, M.; *Org. Magn. Reson.* **1981**, *16*, 82. (k) Reynolds, W. L.; Reichley-Yinger, L.; Yuan, Y. *J. Chem. Soc., Chem. Commun.* **1985**, 526. (l) Reynolds, W. L.; Reichley-Yinger, L.; Yuan, Y. *Inorg. Chem.* **1985**, *24*, 4273.

complex is higher than in the bulk solution. Saturation is observed when most complexes have a solvation sphere that contains the necesary number of acetonitrile molecules. After this bulk concentration (~10 M) is reached, further increases in the bulk concentration of acetonitrile have a smaller effect.

To establish that the complex *is* preferentially solvated in CH_2Cl_2 and to a much lesser extent in CH_3NO_2, ^1H NMR spectra of $[(HMB)Ru(anth)]^{2+}$ were obtained (Table II) for a range of concentrations of CD_3CN in both CD_2Cl_2 and CD_3NO_2. The normalized ^1H NMR resonance positions of the coordinated HMB peak (referenced to TMS) were then plotted vs the acetonitrile concentration (shown in Figure 3). The similarity between the NMR and kinetic data is immediately apparent. The gentle curvature that is observed in the nitromethane data is probably due to a slight residual amount of preferential solvation even in this high dielectric solvent. The difference between the kinetic and NMR data in methylene chloride solutions at higher concentrations of acetonitrile (i.e. the continued shift in the ^1H NMR signal when the maximum k_{obs} has been reached) can be explained by considering that the number of acetonitrile molecules required to form the transition state is less than the total number in the solvation sphere. Once the transition state requirement is met, no further rate increase is observed, but the HMB peak continues to shift as acetonitrile completes the solvation sphere.

Conclusions

We propose a mechanism that is consistent with the kinetic and NMR data for both solvent systems and that takes into account preferential solvation:

$$[(HMB)Ru(anth)]^{2+} + CH_3CN \overset{K}{\rightleftharpoons} [(HMB)Ru(anth)]^{2+}\cdot CH_3CN \quad (7)$$

$$[(HMB)Ru(anth)]^{2+}\cdot CH_3CN \xrightarrow[2CH_3CN]{k_2} [(HMB)Ru(CH_3CN)_3]^{2+} + \text{anthracene} \quad (8)$$

where $K_{CH_2Cl_2} > K_{CH_3NO_2}$ and $k_{2(CH_2Cl_2)} < k_{2(CH_3NO_2)}$. The equilibrium constant K refers to replacement of a solvent molecule in the solvation sphere by CH_3CN while k_2 is the first-order rate constant for the release of anthracene from the preferentially (CH_3CN) solvated complex, $[(HMB)Ru(anth)]^{2+}\cdot CH_3CN$. We plan further work in this area designed to investigate the analogous photochemical reaction of $[(HMB)Ru(anth)]^{2+}$.

Acknowledgment. We thank Professor Warren Reynolds for several stimulating discussions concerning the preferential solvation of ions. D.A.F. acknowledges support from the Sohio-Lando program. This material is based upon work supported in part by the National Science Foundation under Grant No. CHE-8722843. The U.S. Government has certain rights in this material.

Registry No. $[(HMB)Ru(anth)][PF_6]_2$, 122270-02-4; $[RuCl_2(HMB)]_2$, 67421-02-7; anthracene, 120-12-7.

Contribution from the Department of Chemistry, University at Buffalo, State University of New York, Buffalo, New York 14214

Nucleophilicities of the Metal Carbonyl Anions: Effects of Ligands, Solvent, and Countercation

Chung-Kung Lai, William G. Feighery, Yueqian Zhen, and Jim D. Atwood*

Received March 30, 1989

Nucleophilicity has been, and remains, a major focus of organic reactions.[1] The concept has had more limited use in inorganic reactions with the primary focus on metal carbonyl anions.[2,3] The most often used measure of nucleophilicities is the rate of displacement of iodide from MeI. In this note we report the effects of ligand environment, solvent, and countercation on the nucleophilicity of metal carbonyl anions.

Table I. Rate Constants for Reactions of Metal Carbonyl Anions and CH_3I in CH_3CN at 25 °C

complex	CH_3CN^a	glyme[b]	THF[c]
$(PPN)CpFe(CO)_2$	very rapid		2.8×10^6
$(PPN)Re(CO)_5$	74 ± 7	254	1.0×10^3
$(PPN)Mn(CO)_4(PBu_3)$	89 ± 8		
$(PPN)Mn(CO)_4(PEt_3)$	62 ± 4		
$(PPN)Mn(CO)_3(PPh_3)_2$	44 ± 5		
$(PPN)Mn(CO)_4(PPh_2Me)$	19 ± 1		
$(PPN)Mn(CO)_4(PPh_3)$	7.8 ± 0.4		
$(PPN)Mn(CO)_4[P(OPh)_3]$	1.9 ± 0.1		
$(PPN)Mn(CO)_5$	1.5 ± 0.2	0.77	7.4
$(PPN)CpW(CO)_3$	0.51 ± 0.009	5.0	2.4
$(PPN)CpMo(CO)_3$	0.39 ± 0.05	0.67	1.5
$(PPN)CpCr(CO)_3$	0.058 ± 0.005	0.04	0.075
$(PPN)Co(CO)_3(PPh_3)$	0.37 ± 0.004		
$(PPN)Co(CO)_3(PBu_3)$	0.012 ± 0.002		
$(PPN)Co(CO)_4$	0.009 ± 0.001	0.01	0.0437

[a] This work; errors are quoted as 95% confidence limits. [b] Estimated data from ref 3. [c] Na^+ countercation; ref 2.

We have examined the reactions of the metal carbonyl anions[4] listed in Table I with MeI by infrared stopped-flow spectrophotometry.[6,7] The product in each case is the methyl complex, MeM. The reactions are first order in metal carbonyl anion and in MeI.

$$\text{rate} = k[M^-][MeI]$$

The rate constants reported (Table I) are obtained as the slope of plots of pseudo-first-order rate constants, k_{obs}, versus [MeI]. Representative data are given in the supplemental data. The rates of reaction of some of the metal carbonyl anions with MeI have been previously reported and are also listed in Table I.[2,3] Considering the difference in solvent and counterion, the three studies show reasonable agreement in rates and agreement in the order of nucleophilicities:

$$Co(CO)_4^- < CpCr(CO)_3^- < CpMo(CO)_3^- < Mn(CO)_5^- < Re(CO)_5^- < CpFe(CO)_2^-$$

As shown by the data in Table II, the nucleophilicity is relatively unaffected by changes in solvent. The data also show a rather small effect of the countercation with a slower rate for the more interacting cation.

(1) See for instance: (a) Bunnett, J. F. *Annu. Rev. Phys. Chem.* **1963**, *14*, 271. (b) Ritchie, C. D. *Acc. Chem. Res.* **1972**, *5*, 348. (c) Bordwell, F. G.; Hughes, D. L. *J. Org. Chem.* **1983**, *48*, 2206. (d) Eberson, L. *Acta Chem. Scand.* **1984**, *B38*, 439. (e) Jencks, W. P.; Gilchrist, M. *J. Am. Chem. Soc.* **1968**, *90*, 2622. (f) Bordwell, F. G.; Harrelson, J. A., Jr. *J. Am. Chem. Soc.* **1989**, *111*, 1052.
(2) Pearson, R. G.; Figdore, P. E. *J. Am. Chem. Soc.* **1980**, *102*, 1541.
(3) Dessy, R. E.; Pohl, R. L.; King, R. B. *J. Am. Chem. Soc.* **1966**, *88*, 5121.
(4) The metal carbonyl anions were prepared as previously described.[5]
(5) (a) Lai, C. K.; Atwood, J. D. Submitted for publication. (b) Zhen, Y.; Atwood, J. D. *J. Am. Chem. Soc.* **1989**, *111*, 1506. (c) Zhen, Y.; Feighery, W. G.; Lai, C. K.; Atwood, J. D. *J. Am. Chem. Soc.*, in press.
(6) Corraine, M. S.; Atwood, J. D. *Inorg. Chem.*, in press.
(7) All the kinetic experiments were performed on an IR stopped-flow spectrophotometer as described previously.[6] All reactions that had been previously[2,3,8] shown to be second order were run under pseudo-first-order conditions with excess alkyl halide. Typical concentrations of metal anion and CH_3I for kinetic studies were 0.001–0.010 and 0.01–10.0 M in CH_3CN at 25 °C, depending on the reaction rates of different metal anions. The rates were monitored by the observed decrease in intensity of the infrared absorbance at 1865, 1860, 1794, 1790, 1751, 1805, 1807, 1830, 1830, 1860, 1788, 1768, 1886, and 1880 cm^{-1} for the metal anions $CpFe(CO)_2^-$, $Re(CO)_5^-$, $Mn(CO)_4(PBu_3)^-$, $Mn(CO)_4(PEt_3)^-$, $Mn(CO)_3(PPh_3)_2^-$, $Mn(CO)_4(PPh_2Me)^-$, $Mn(CO)_4(PPh_3)^-$, $Co(CO)_3(PPh_3)^-$, $Mn(CO)_4[P(OPh)_3]^-$, $Mn(CO)_5^-$, $CpMo(CO)_3^-$, $CpCr(CO)_3^-$, $Co(CO)_3(PBu_3)^-$, and $Co(CO)_4^-$, respectively. The observed rate constants, the standard deviation, and the error at the chosen confidence limit were calculated by using the OLIS computer programs.[6] The second-order rate constants, k, were obtained as the slope of plots of k_{obs} versus $[CH_3I]$.
(8) (a) Darensbourg, M. Y.; Darensbourg, D. J; Burns, D.; Drew, D. A. *J. Am. Chem. Soc.* **1976**, *98*, 3127. (b) Gladysz, J. A.; Williams, G. M.; Tam, W.; Johnson, D. L.; Parker, D. W.; Selover, J. C. *Inorg. Chem.* **1979**, *18*, 553. (c) Darensbourg, M. Y.; Jimenez, P.; Sackett, J. R.; Hanckel, J. M.; Kump, R. L. *J. Am. Chem. Soc.* **1982**, *104*, 1521.

0020-1669/89/1328-3929$01.50/0